



A image encryption algorithm based on chaotic Lorenz system and novel primitive polynomial S-boxes

Temadher Alassiry Al-Maadeed¹ · Iqtadar Hussain¹ · Amir Anees² ·
Muhammad Tahir Mustafa¹

Received: 30 June 2020 / Revised: 25 January 2021 / Accepted: 10 February 2021 /

Published online: 12 April 2021

© The Author(s) 2021

Abstract

We have proposed a robust, secure and efficient image encryption algorithm based on chaotic maps and algebraic structure. Nowadays, the chaotic cryptosystems gained more attention due to their efficiency, the assurance of robustness and high sensitivity corresponding to initial conditions. In literature, there are many encryption algorithms that can simply guarantees security while the schemes based on chaotic systems only promises the uncertainty, both of them can not encounter the needs of current scenario. To tackle this issue, this article proposed an image encryption algorithm based on Lorenz chaotic system and primitive irreducible polynomial substitution box. First, we have proposed 16 different S-boxes based on projective general linear group and 16 primitive irreducible polynomials of Galois field of order 256, and then utilized these S-boxes with combination of chaotic map in image encryption scheme. Three chaotic sequences can be produced by the disturbed of Lorenz chaotic system corresponding to variables x , y and z . We have constructed a new pseudo random chaotic sequence k_i based on x , y and z . The plain image is encrypted by the use of chaotic sequence k_i and XOR operation to get a ciphered image. To show the strength of presented image encryption, some renowned analyses are performed.

Keywords Lorenz System · Chaos · Substitution box · Image encryption · Cryptanalysis

✉ Temadher Alassiry Al-Maadeed
t.alassiry@qu.edu.qa

Iqtadar Hussain
iqtadarqau@qu.edu.qa

Amir Anees
a.anees@deakin.edu.au

Muhammad Tahir Mustafa
tahir.mustafa@qu.edu.qa

¹ Department of Mathematics, Statistics and Physics, College of Arts and Science, Qatar University, Doha, 2713, Qatar

² School of Info Technology, Faculty of Science, Engineering and Built Environment, Deakin University, Melbourne, Australia

1 Introduction

Substitution box (S-box) is one of the fundamental constitute of symmetric key algorithms which implement substitution. Substitution boxes are building blocks of symmetric cryptosystems. The substitution tables (S-boxes) play a vital role in the encryption algorithms in order to meet the definition of a perfect security. Sometime big structures like S-box slow-down the processing of the encryption in a scenario where big data processing is required, the main reason is the complexity of that system and this kind of negative effect reduce the utility of that encryption algorithm in practical communication. In literature, there are many chaotic schemes that are using one or multiple (S-boxes) to get more security, there is no doubt that when one will use S-box the confusion creating ability of that algorithm between ciphertext and secret key will improve but it will definitely slow down the speed of encryption [6, 9, 10, 13, 18, 23, 24, 27, 29, 33–36, 39–41]. In this paper, we have proposed an image encryption algorithm that is based on chaotic maps and S-boxes. First, we have proposed a novel 16 different S-boxes based on 16 different primitive irreducible polynomials of Galois field of order 256 and project general linear group, then we used proposed S-boxes in image encryption. The proposed work is to construct a secure and efficient image encryption scheme based on straightforward and little complex steps, by chaotic Lorenz system.

1.1 Related work

Last decade is considered as a remarkable era for secure communication and image processing. In wireless communication, protection of digital data such as text, sound, image and video has more importance because multimedia kind of stuff has taken hold on many important fields like electronic commerce, banking industry, law enforcement agencies requirements and personal data. The performance of old cryptosystems for image is poor in encryption of bulk sized data [44, 45]. To tackle this problem, new schemes based on chaos for image encryption have been developed.

In [3, 17], Amigo et al., and Jakimoski, has shown a link between secure communication and chaos theory. They said chaotic maps could achieve some basic requirements of secure communication such as randomness, robustness and sensitivity to initial conditions. In [2, 28], Ott and Alvarez has observed that values breded by chaotic maps can be regained based on initial conditions but extremely erratic, and this kind of behavior is valuable for cryptosystems. Based on these properties, some cryptographers has proposed novel cryptosystems in [11, 31]. Pseudorandom number generator based on chaotic maps is one of the emerging field nowadays and can be utilized in different cryptosystems to get more security [30]. In [21], the virtual analysis of Advanced Encryption Standard (AES), Data Encryption Standard (DES) and 3DES are presented. The scrutiny of AES is explained considering the high throughput, area efficiency and elevated performance [20, 46]. It is presented that AES is as authorized Advance Encryption standard (AES) and it is well apt for hardware exercise. Moreover, the work described how to minimize the power dissipation and how to map the S-box into prototype chip. Further, the work highlighted the secure components of S-box which is using XOR operations instead of polynomial multiplication still there is a limitation of complex look up tables that were used in the creation of S-box. In [14], the cryptanalysis of previously published cryptosystem is presented. The already previously published cryptosystem was based on the on iterating chaotic map. It is shown in [14] that this previously published cryptosystem is weak and can easily be broken. To strengthen it, [14] proposed novel improvements to the proposed chaotic cryptosystem.

The rest of paper is arranged as follows: Some basic definitions of mathematical background for cryptography and details of chaotic map are given in Section 2. The detailed description of proposed image encryption algorithm is given Section 3. Section 4 depicts the results of simulation and different analyses. The conclusion of whole scheme is given in Section 5.

2 Basic definitions

In this section, the structural units of proposed image encryption technique are briefly discussed. First, an introduction to the Galois field and its primitive irreducible polynomials is presented followed with the basics of Projective General Linear Group. Secondly, the comprehensive description of chaotic Lorenz map is discussed in this section.

2.1 Galois field and its primitive irreducible polynomials

From the knowledge of Galois field, we can say that if p is a non-zero element of a Principle Ideal Domain (PID) \mathbf{R} , then $\frac{\mathbf{R}}{p}$ will be a field if p is irreducible. Therefore, for a prime p and $q = p^n$, we can denote the finite field of order q as $\mathbf{GF}(q) = \mathbf{GF}(p^n)$. The polynomial extension $\mathbf{R}[x]$ of intergral domanin \mathbf{R} is also intergral domain, therefore, in case of polynomial extension $\mathbf{R}[x]/\langle p(x) \rangle$ will be a field structure when $p(x)$ is primitive irreducible polynomial, where $\langle p(x) \rangle$ is a maximal ideal.

$$\mathbf{GF}(q) = \frac{\mathbf{GF}(p)[x]}{\langle m(x) \rangle} \tag{1}$$

Where $m(x)$ is monic primitive irreducible polynomial of degree n in Galois field $\mathbf{GF}(p^n)$. The example of above formula is as follows:

$$\mathbf{GF}(2^8) = \frac{\mathbf{GF}(2)[x]}{\langle x^8 + x^7 + x^6 + x^5 + x^4 + x^2 + 1 \rangle} \tag{2}$$

$$\mathbf{GF}(2^8) = \left\{ a_1 + a_2x + a_3x^2 + a_4x^3 + a_5x^4 + a_6x^5 + a_7x^6 + a_8x^7 + \langle m(x) \rangle \mid a_i \in \mathbf{GF}(2) \right\} \tag{3}$$

The elements of $\mathbf{GF}(2^8)$ can be represented by a polynomial of degree 8 and $\langle m(x) \rangle$ is the maximal ideal generated by monic irreducible polynomial, when the degree of polynomial will exceed from 7 this maximal ideal will absorb it. Now, the question is how many different irreducible polynomials are there corresponding to any Galosi field $\mathbf{GF}(p^n)$. The formula to find all irreducible polynomials is as follows:

$$\frac{1}{n} \sum_{d|n} \mu(d) P^{n/d} \tag{4}$$

By using above formula, it can be seen in Table 1, that there are 30 irreducible polynomials for $\mathbf{GF}(2^8)$. But for the construction of Galosi field which can generate its non-zero elements we need primitive irreducible polynomials. In Table 1, we have shown that out of 30 irreducible polynomials 16 are primitive irreducible. We have used Rabin’s test to find 30 irreducible polynomials, Rabin’s test is as follows:

Theorem 1 *Let p_1, p_2, \dots, p_k be all the prime divisors of n , and denoted $n_i = n/p_i$, for $1 \leq i \leq k$. A polynomial $f \in \mathbf{F}_q[x]$ of defree n is irreducible in $\mathbf{F}_q[x] \Leftrightarrow \gcd(f, x^{q^{n_i}} - x \bmod f) = 1$ for $1 \leq i \leq k$, and f divides $x^{q^n} - x$.*

Table 1 Irreducible and primitive irreducible polynomials corresponding to $\mathbf{GF}(2^8)$

8 degree polynomials of $\mathbf{GF}(2^8)$	Irreducible	Prim. irreducible
$x^8 + x^7 + x^5 + x^4 + 1$	Yes	No
$x^8 + x^4 + x^3 + x^2 + 1$	Yes	Yes
$x^8 + x^5 + x^3 + x^1 + 1$	Yes	Yes
$x^8 + x^7 + x^6 + x^4 + x^3 + x^2 + 1$	Yes	No
$x^8 + x^6 + x^5 + x^4 + x^2 + x^1 + 1$	Yes	No
$x^8 + x^7 + x^6 + x^5 + x^4 + x^3 + 1$	Yes	No
$x^8 + x^5 + x^3 + x^2 + 1$	Yes	Yes
$x^8 + x^6 + x^4 + x^3 + x^2 + x^1 + 1$	Yes	Yes
$x^8 + x^4 + x^3 + x + 1$	Yes	No
$x^8 + x^7 + x^6 + x^1 + 1$	Yes	Yes
$x^8 + x^6 + x^5 + x^2 + 1$	Yes	Yes
$x^8 + x^6 + x^5 + x^4 + x^3 + x^1 + 1$	Yes	No
$x^8 + x^7 + x^2 + x^1 + 1$	Yes	Yes
$x^8 + x^7 + x^5 + x^4 + x^3 + x^2 + 1$	Yes	No
$x^8 + x^7 + x^3 + x^2 + 1$	Yes	Yes
$x^8 + x^7 + x^6 + x^5 + x^4 + x^2 + 1$	Yes	Yes
$x^8 + x^5 + x^4 + x^3 + x^2 + x^1 + 1$	Yes	No
$x^8 + x^7 + x^6 + x^5 + x^2 + x^1 + 1$	Yes	Yes
$x^8 + x^7 + x^6 + x^4 + x^2 + x^1 + 1$	Yes	No
$x^8 + x^6 + x^3 + x^2 + 1$	Yes	Yes
$x^8 + x^7 + x^4 + x^3 + x^2 + x^1 + 1$	Yes	No
$x^8 + x^7 + x^6 + x^3 + x^2 + x^1 + 1$	Yes	Yes
$x^8 + x^7 + x^6 + x^5 + x^4 + x^1 + 1$	Yes	No
$x^8 + x^6 + x^5 + x^1 + 1$	Yes	Yes
$x^8 + x^5 + x^4 + x^3 + 1$	Yes	No
$x^8 + x^6 + x^5 + x^3 + 1$	Yes	Yes
$x^8 + x^7 + x^5 + x^1 + 1$	Yes	No
$x^8 + x^6 + x^5 + x^4 + 1$	Yes	Yes
$x^8 + x^7 + x^3 + x^1 + 1$	Yes	No
$x^8 + x^7 + x^5 + x^3 + 1$	Yes	Yes

A primitive polynomial is a polynomial that generates all elements of an extension field from a base field. Primitive polynomials are also irreducible polynomials. For any prime or prime power q and any positive integer n , there exists a primitive polynomial of degree n over $\mathbf{GF}(q)$. There are

$$a_q(n) = \frac{\phi(q^n - 1)}{n} \tag{5}$$

primitive polynomials over $\mathbf{GF}(q)$, where $\phi(n)$ is the totient function.

Theorem 2 A polynomial of degree n over the finite field $\mathbf{GF}(2)$ is primitive if it has polynomial order $2^n - 1$.

Theorem 1, gave us 30 irreducible polynomial of Table 1. Now, the question is how to get 16 primitive irreducible polynomials from 30 irreducible polynomials. To explain this procedure, we have considered an example of $GF(2^4)$.

$$GF(2^4) = \frac{GF(2)[x]}{(x^4 + x^3 + 1)} \tag{6}$$

There are two primitive irreducible polynomials for $GF(2^4)$. The process to check whether an irreducible polynomial is primitive irreducible or not is shown in the example and counter example below.

Let $f(x) = x^4 + x^3 + 1$ is an irreducible polynomial. suppose α is the root of $f(x)$. If α is the root of $f(x)$ then we have

$$f(\alpha) = \alpha^4 + \alpha^3 + 1 = 0 \tag{7}$$

$$\alpha^4 = \alpha^3 + 1 \tag{8}$$

Because the coefficients of polynomial are in $GF(2)$, that is why $-1 = +1$.

$$\alpha^5 = \alpha^4 + \alpha = \alpha^3 + 1 + \alpha = \alpha^3 + \alpha + 1 \tag{9}$$

$$\alpha^6 = \alpha^4 + \alpha^2 + \alpha = \alpha^3 + 1 + \alpha^2 + \alpha = \alpha^3 + \alpha^2 + \alpha + 1 \tag{10}$$

$$\alpha^7 = \alpha^4 + \alpha^3 + \alpha^2 + \alpha = \alpha^3 + 1 + \alpha^3 + \alpha^2 + \alpha = \alpha^2 + \alpha + 1 \tag{11}$$

Where $2\alpha^3 = 0$ due to $GF(2)$.

$$\alpha^8 = \alpha^3 + \alpha^2 + \alpha \tag{12}$$

$$\alpha^9 = \alpha^4 + \alpha^3 + \alpha^2 = \alpha^3 + 1 + \alpha^3 + \alpha^2 = \alpha^2 + 1 \tag{13}$$

$$\alpha^{10} = \alpha^3 + \alpha \tag{14}$$

$$\alpha^{11} = \alpha^4 + \alpha^2 = \alpha^3 + 1 + \alpha^2 = \alpha^3 + \alpha^2 + 1 \tag{15}$$

$$\alpha^{12} = \alpha^4 + \alpha^3 + \alpha = \alpha^3 + 1 + \alpha^3 + \alpha = \alpha + 1 \tag{16}$$

$$\alpha^{13} = \alpha^2 + \alpha \tag{17}$$

$$\alpha^{14} = \alpha^3 + \alpha^2 \tag{18}$$

$$\alpha^{15} = \alpha^4 + \alpha^3 = \alpha^3 + 1 + \alpha^3 = 1 \tag{19}$$

It can be seen in above example that we are getting $\alpha^{15} = 1$, and the order of $GF(2^4)$ is 16, it means $f(x) = x^4 + x^3 + 1$ is a primitive polynomial because it is generating all non-zero elements of $GF(2^4)$. Where α the root of primitive polynomial is known as primitive element, in other words, because GF is also a cyclic group so α is the generator. All irreducible polynomials are not primitive, to show this fact a counter example is as follows:

Let $f'(x) = x^4 + x^2 + 1$ is an irreducible polynomial. suppose β is the root of $f(x)$. If β is the root of $f'(x)$ then we have

$$f'(\beta) = \beta^4 + \beta^2 + 1 = 0 \tag{20}$$

$$\beta^4 = \beta^2 + 1 \tag{21}$$

Because the coefficients of polynomial are in $GF(2)$, that is why $-1 = +1$.

$$\beta^5 = \beta^3 + \beta \tag{22}$$

$$\beta^6 = \beta^4 + \beta^2 = \beta^2 + 1 + \beta^2 = 2\beta^2 + 1 = 1 \tag{23}$$

It can be seen that $f'(x) = x^4 + x^2 + 1$ is irreducible but not primitive, because it is not generating all non-zero elements of $GF(2^4)$. Similarly, in Table 1, we have got all primitive irreducible polynomials form irreducible polynomials.

2.2 Projective General Linear group (PGL)

The Projective General Linear Group (PGL) can be defined as the group acting on $\bar{F} = \mathbf{GF}(p^n) \cup \{\infty\}$ is the group of all transformations and is denoted by $PGL(2, \mathbf{GF}(p^n))$. With the standard understanding about ∞ , $PGL(2, \mathbf{GF}(p^n))$ is the set of all linear fractional transformations (LFT) of $\bar{F} = \mathbf{GF}(p^n) \cup \{\infty\}$,

$$PGL(2, \mathbf{GF}(p^n)) = \left\{ g : \bar{F} \rightarrow \bar{F} \mid g(z) = \frac{az + b}{cz + d}, a, b, c, d \in \mathbf{GF}(p^n), ad - bc \neq 0 \right\} \tag{24}$$

Linear fractional transformation $g(z)$ is shortly denoted by LFT. We study a special class of maps

$$f : PGL(2, \mathbf{GF}(2^8)) \times \mathbf{GF}(2^8) \rightarrow \mathbf{GF}(2^8) \tag{25}$$

A LFT of $PGL(2, \mathbf{GF}(2^8)) \times \mathbf{GF}(2^8)$ is a map of the form $g(z) = \frac{az+b}{cz+d}$, $a, b, c, d \in \mathbf{GF}(2^8)$ and $ad - bc \neq 0$

Transformation is depending on the invertible 2×2 matrix $\begin{pmatrix} a & b \\ c & d \end{pmatrix}$

2.3 Chaotic Lorenz system

The idea to define the chaotic dynamics with the help of chaotic maps is a big breakthrough in the filed of dynamical systems. In the atmosphere, the mathematical modelling of the air flow was first presented by E. Lorenz [10, 23]. The system of chaotic differential equation is given as

$$\frac{dx}{dt} = a(y - x) \tag{26}$$

$$\frac{dy}{dt} = bx - y - xz \tag{27}$$

$$\frac{dz}{dt} = xy - cz \tag{28}$$

Where the intervals for variables x, y and z are given $-60 \leq x \leq 60, -60 \leq y \leq 60, -60 \leq z \leq 60$. For chaotic behavior, the values for parameters a, b , and c are $a = 10, b = 28$ and $c = 8/3$ respectively.

3 Primitive irreducible polynomial S-boxes

Now from the above linear transforamtion, we have;

$$f_i : PGL \left(2, GF(2^8) = \frac{GF(2)[x]}{\langle p_i(x) \rangle} \right) \times \left(GF(2^8) = \frac{GF(2)[x]}{\langle p_i(x) \rangle} \right) \rightarrow \left(GF(2^8) = \frac{GF(2)[x]}{\langle p_i(x) \rangle} \right) \tag{29}$$

Where $p_i(x), i = 1, 2, 3, \dots, 16$ are set of primitive irreducible polynomials of Table 1 for $GF(2^8)$. Therefore, we have 16 different f_i , where $i = 1, 2, 3, \dots, 16$ to construct 16 different S-boxes with fixed $a, b, c, d \in GF(2^8)$. The order of $PGL(2, GF(2^8))$ is 16776960, therefore one can construct huge number of S-boxes by changing $a, b, c, d \in GF(2^8)$. In this section, we have given an example for the construction of one S-box based on

$a = 32, b = 22, c = 11, d = 8 \in GF(2^8)$ and $p_1(x) = x^8 + x^4 + x^3 + x^2 + 1$. In polynomial form, $a = x^5, b = x^4 + x^2 + x, c = x^3 + x + 1, d = x^3$. Here it must be noted that the sign '+' indicates XOR operation.

$$f_1(z) = \frac{(x^5)(z) + (x^4 + x^2 + x)}{(x^3 + x + 1)(z) + (x^3)} \tag{30}$$

For $z = 0$

$$f_1(0) = \frac{(x^5)(0) + (x^4 + x^2 + x)}{(x^3 + x + 1)(0) + (x^3)} = \frac{x^4 + x^2 + x}{x^3} = \frac{\mu^{239}}{\mu^3} = \mu^{239-3-1} = \mu^{237} = 237 \tag{31}$$

Where $\mu^{239} = \mu^4 + \mu^2 + \mu, \mu^3 = x^3$ based on $p_1(x) = x^8 + x^4 + x^3 + x^2 + 1$, corresponding to different primitive polynomials $p_i(x)$ of $GF(2^8)$ these values of μ power will be different.

For $z = 1$

$$\begin{aligned} f_1(1) &= \frac{(x^5)(1) + (x^4 + x^2 + x)}{(x^3 + x + 1)(1) + (x^3)} = \frac{x^5 + x^4 + x^2 + x}{2x^3 + x + 1} \\ &= \frac{x^5 + x^4 + x^2 + x}{x + 1} = \frac{\mu^{249}}{\mu^{25}} = \mu^{249-25-1} = \mu^{225} = 225 \end{aligned} \tag{32}$$

Where $\mu^{249} = \mu^5 + \mu^4 + \mu^2 + \mu, \mu^{25} = \mu + 1$ based on $p_1(x) = x^8 + x^4 + x^3 + x^2 + 1$

For $z = 2$

$$\begin{aligned} f_1(2) &= \frac{(x^5)(2) + (x^4 + x^2 + x)}{(x^3 + x + 1)(2) + (x^3)} = \frac{(x^5)(x) + (x^4 + x^2 + x)}{(x^3 + x + 1)(x) + (x^3)} = \frac{x^6 + x^4 + x^2 + x}{x^4 + x^3 + x^2 + x} \\ &= \frac{x^5 + x^4 + x^2 + x}{x + 1} = \frac{\mu^{219}}{\mu^{76}} = \mu^{219-76-1} = \mu^{144} = 144 \end{aligned} \tag{33}$$

Where $\mu^{219} = \mu^6 + \mu^4 + \mu^2 + \mu, \mu^{76} = \mu^4 + \mu^3 + \mu^2 + \mu$ based on $p_1(x) = x^8 + x^4 + x^3 + x^2 + 1$. Similarly, for $z = 3, 4, 5, \dots, 255$ all the elements can be constructed corresponding to primitive irreducible polynomial $p_1(x) = x^8 + x^4 + x^3 + x^2 + 1$. All elements of $p_1(x)$ S-box are shown in Table 2.

3.1 Analysis for evaluating the strength of S-box

In the analysis section, we shall determine the cryptographic strength of the propose S-box with some suitable measures. To find the S-box with fitting confusion creating strength many standard evaluating analysis are presented in literature such as Non-linearity, Bit independent criterion (BIC), Strict avalanche criterion (SAC), Linear approximation probability (LP) and Differential approximation probability (DP). We shall also use these criteria to test the security of proposed S-box.

To measure the good properties of S-box benchmark criteria are presented in literature like bijectivity, differential approximation probability (DP), strict avalanche criterion (SAC), bit independence criterion (BIC), nonlinearity, and linear probability (LP). We carry out the security analysis of the proposed S-box of example given in Table 2 using these well known criteria.

1. Bijectivity: [16, 22] If the linear sum of the Boolean function f_i of each component of the designed $n \times n$ S-box is 2^{n-1} , then f is a bijection. Mathematically, we can write as

$$wt(a_1 f_1 + a_2 f_2 + \dots + a_n f_n). \tag{34}$$

Table 2 The proposed S-box

	0	1	2	3	4	5	6	7	8	9	10	11	12	13	14	15
0	237	225	144	236	211	25	147	20	185	127	132	195	123	136	197	170
1	109	112	61	84	183	4	186	54	234	121	177	129	215	48	41	1
2	162	228	194	150	141	175	74	91	70	50	47	85	176	40	34	102
3	119	223	202	206	7	22	98	158	190	148	69	30	38	113	179	224
4	131	104	165	178	106	169	174	116	26	154	21	90	65	157	76	64
5	45	5	253	86	172	124	180	67	247	115	42	118	217	240	189	192
6	199	12	6	125	216	254	251	231	210	227	126	160	151	107	73	139
7	77	122	188	8	16	232	153	111	143	203	24	39	95	99	78	182
8	89	213	241	171	81	9	72	13	105	205	3	59	120	245	35	168
9	137	27	66	97	79	71	55	226	201	187	214	239	80	2	208	255
10	63	156	249	135	83	248	110	140	29	163	155	219	184	49	68	173
11	200	10	149	51	23	57	157	14	94	58	15	209	18	103	193	142
12	133	11	56	181	242	43	96	196	33	229	37	220	130	60	88	212
13	46	93	44	221	62	87	114	100	75	246	230	222	204	235	19	164
14	128	233	252	117	82	146	138	17	161	191	53	218	166	52	145	23
15	159	108	198	28	92	31	243	207	32	134	244	0	250	152	36	101

where $a_i \in 0, 1, (a_1, a_2, \dots, a_n) \neq (0, 0, \dots, 0)$, $wt()$ denotes the Hamming weight. In effect, an inverse is important specifically in a substitution network, therefore S-box should be bijective.

2. Nonlinearity: The nonlinearity of an S-box can be tested by the following formula:

$$N_f = 2^{-n} \left(1 - \max_{\omega \in GF(2^n)} \left| 2^{-n} \sum_{x \in GF(2^n)} (-1)^{f(x) \oplus x \cdot \omega} \right| \right), \tag{35}$$

where $\omega \in GF(2^8)$.

3. Strict avalanche criterion: This analysis depicts information that while one bit of eight lengths input byte of plaintext modifies, will yield a 0.5 probability of the outcomes changes in byte of 8 bits balanced for entries.
4. Bit independent criterion: For two Boolean function f_j, f_k , one can test the independence criterion of a substitution box by validating if, for any two output bits of the S-box, $f_j \oplus f_k (j \neq k)$ fulfills the SAC and nonlinearity.
5. XOR table and differential invariant: XOR table of substitution box basically depends on the calculation of $\rho_L(a, b) = \{x \in GF(2^8) : L(x) \oplus L(a \oplus x) = M\} \forall a, b \in GF(2^8)$. The differential invariant $\rho_L(a, b)$ is found as follows:

$$\rho_L(a, b) = \max_{a, b \in GF(2^8), a \neq 0} |\{x \in GF(2^8) : L(x) \oplus L(a \oplus x) = M\}|.$$

Table 3 presents the results of above discussed analysis for our proposed S-boxes with different Primitive polynomial of $GF(2^8)$.

Table 3 Analysis of proposed S-boxes with different Primitive polynomial of $GF(2^8)$

Pri. poly of $GF(2^8)$	N.L	BIC	BIC of SAC	SAC	LP	DP
$x^8 + x^4 + x^3 + x^2 + 1$	104.75	105.071	0.500	0.493	160/ 0.125	0.125
$x^8 + x^5 + x^3 + x^1 + 1$	105.75	104.929	0.502	0.503	158/ 0.140	0.242
$x^8 + x^5 + x^3 + x^2 + 1$	104.75	101.14	0.502	0.497	168/ 0.156	0.5
$x^8 + x^6 + x^4 + x^3 + x^2 + x^1 + 1$	105.75	105.35	0.502	0.502	160/0.125	0.125
$x^8 + x^7 + x^6 + x^1 + 1$	104.5	104.14	0.498	0.498	164/0.148	0.25
$x^8 + x^6 + x^5 + x^2 + 1$	105.5	105.71	0.502	0.505	160/0.125	0.125
$x^8 + x^7 + x^2 + x^1 + 1$	106.75	104.85	0.503	0.502	160/0.125	0.125
$x^8 + x^7 + x^3 + x^2 + 1$	104.25	104.42	0.501	0.512	162/0.132	0.25
$x^8 + x^7 + x^6 + x^5 + x^4 + x^2 + 1$	106.5	105	0.504	0.496	162/0.132	0.117
$x^8 + x^7 + x^6 + x^5 + x^2 + x^1 + 1$	106.25	103.71	0.500	0.498	162/0.132	0.125
$x^8 + x^6 + x^3 + x^2 + 1$	106	105.71	0.501	0.499	158/ 0.125	0.125
$x^8 + x^7 + x^6 + x^5 + x^2 + x^1 + 1$	106	103.57	0.502	0.497	166/0.156	0.25
$x^8 + x^6 + x^5 + x^1 + 1$	106.5	105.5	0.502	0.510	162/ 0.132	0.125
$x^8 + x^6 + x^5 + x^3 + 1$	106.25	105.37	0.504	0.507	158/0.132	0.125
$x^8 + x^6 + x^5 + x^4 + 1$	107.25	106.07	0.5	0.496	158/0.125	0.117
$x^8 + x^7 + x^5 + x^3 + 1$	106	105.35	0.503	0.516	162/0.132	0.125

4 Proposed algorithm for image encryption cryptosystem

In order to encrypt the digital information, we need to design a pseudorandom sequence generator to transform the real solves of chaotic Lorenz system to a digital sequence. The details are represented as follows. From the above system, we can get three real sequences denoted as x , y and z . In order to achieve to a better randomness, we cut off the first N values of the real sequences. Here we set $N = 100$ and denote the three real sequences as $\{x_i\}$, $\{y_i\}$, $\{z_i\}$, where $i = 1, 2, 3, \dots, m \times n$, where $m \times n$ is the size of plain image. The t^{th} value of the sequences of x , y , and z are defined as x_t , y_t and z_t . A disturbing procession is added to avoid the appearance of the periodic absolutely. That is, change the value of x and y with an interval of 10000:

$$\begin{cases} x_t = x_t + 0.1, y_t = y_t - 0.2, & \text{if } z_t \leq 0, t \equiv 1 \pmod{10000}, \\ x_t = x_t + 0.2, y_t = y_t - 0.1, & \text{if } z_t > 0, t \equiv 1 \pmod{10000}. \end{cases} \tag{36}$$

First, we discard the integral part of the real sequences for all of x , y and z :

$$\begin{cases} x_i = x_i - \text{floor}(x_i), \\ y_i = y_i - \text{floor}(y_i), i = 1, 2, 3, \dots, m \times n, \\ z_i = z_i - \text{floor}(z_i). \end{cases} \tag{37}$$

Where $\text{floor}(x)$ denotes the maximum integer that is smaller than x . Second, develop a new chaotic sequence as following:

$$k_i = x_i, y_i, z_i, x_{i+1}, y_{i+1}, z_{i+1}, \dots, x_{i+\text{floor}(\frac{m \times n}{3})}, y_{i+\text{floor}(\frac{m \times n}{3})}, z_{i+\text{floor}(\frac{m \times n}{3})} \tag{38}$$

At last, we get the modified chaotic sequence k_i , the beauty of proposed chaotic sequence is that it has the flavor of three x_i , y_i and z_i chaotic sequences of chaotic Lorenz system.

During experiment we have changed the length of k_i according to the size of plain image $m \times n$ by discarding some of its values from the end.

In order to get an improved image encryption scheme, we have changed the position of plaintext image pixels by randomness of k_i . The proposed scheme consists of two phases, first phase starts from equation 4 and ends at equation 8. The basic purpose of first phase is to changed the pixel positions of image. The second phase consists of equation (9), (10) and (11) and in this process we are attaining pixel value change based on XOR operation to get a fully encrypted image. Let us suppose that the plain image is I with m rows and n columns. For the sake of convince, we have changed the image I to a one dimensional vector, say $I_1(1 :m \times n)$.

$$I_1((p - 1)n + q) = I(p, q) \tag{39}$$

where $p = 1, 2, 3, \dots, m$ and $q = 1, 2, 3, \dots, n$. Now, the chaotic sequence k_i , will change the vector I_1 to I_2 with the help of following procedure.

$$I_2(i) = I_1(k_i) \tag{40}$$

where $i = 1, 2, 3, \dots, m \times n$. Define a new sequence with elements from $GF(2^8)$ based on k_i as follows.

$$l(i) = \text{mod}(\text{round}((k_i \times 10^4)), 256) \tag{41}$$

After getting $l(i)$ sequence of random decimal numbers from $GF(2^8)$. We will XOR $l(i)$ with $I_2(i)$ to get the final vector $I_3(i)$. Reshape $I_3(i)$ in the form of $m \times n$ matrix to get the first level ciphered image as shown in equation (11).

$$I_3(i) = I_2(i) \oplus l(i) \tag{42}$$

$$C.I = \text{reshape}(I_3(i), m, n). \tag{43}$$

As a last step for the proposed algorithm, we have applied the substitution step. We can define the process of substitution in following steps:

1. Consider the pixel of the image in the form of binary byte i.e., 8 binary bits. We divide this set into four LSBs (Least significant bits) and Most significant bits (MSBs).
2. In the next step, the MSBs and LSBs having 4 bits each are converted into decimal values. Conventionally, the pixel value which has to be replaced by S-box value is selected with the help of decimal value of LSBs and MSBs. The column of S-box is selected by the decimal value of LSBs whereas the row of S-box is carefully chosen by decimal value of MSBs.
3. One by one all the pixel values are substituted with the values of S-box.
4. In this case, as there are number of S-boxes so each pixel of the image is replaced by single S-box, second pixel value is replaced by another S-box and this procedure will continue till last pixel value.
5. For the selection of S-box out of 256 S-boxes with whom the original value will be replaced is done with the help of x, y, z trajectories of Lorenz map. The proposed algorithm in the form of a flowchart is shown in Fig. 1.

5 Simulation results and statistical analysis

For simulation results, we take an image of cameraman having size 256×256 . Table 4 represents the initial values of the chaotic maps which are used as secret keys. The plain image

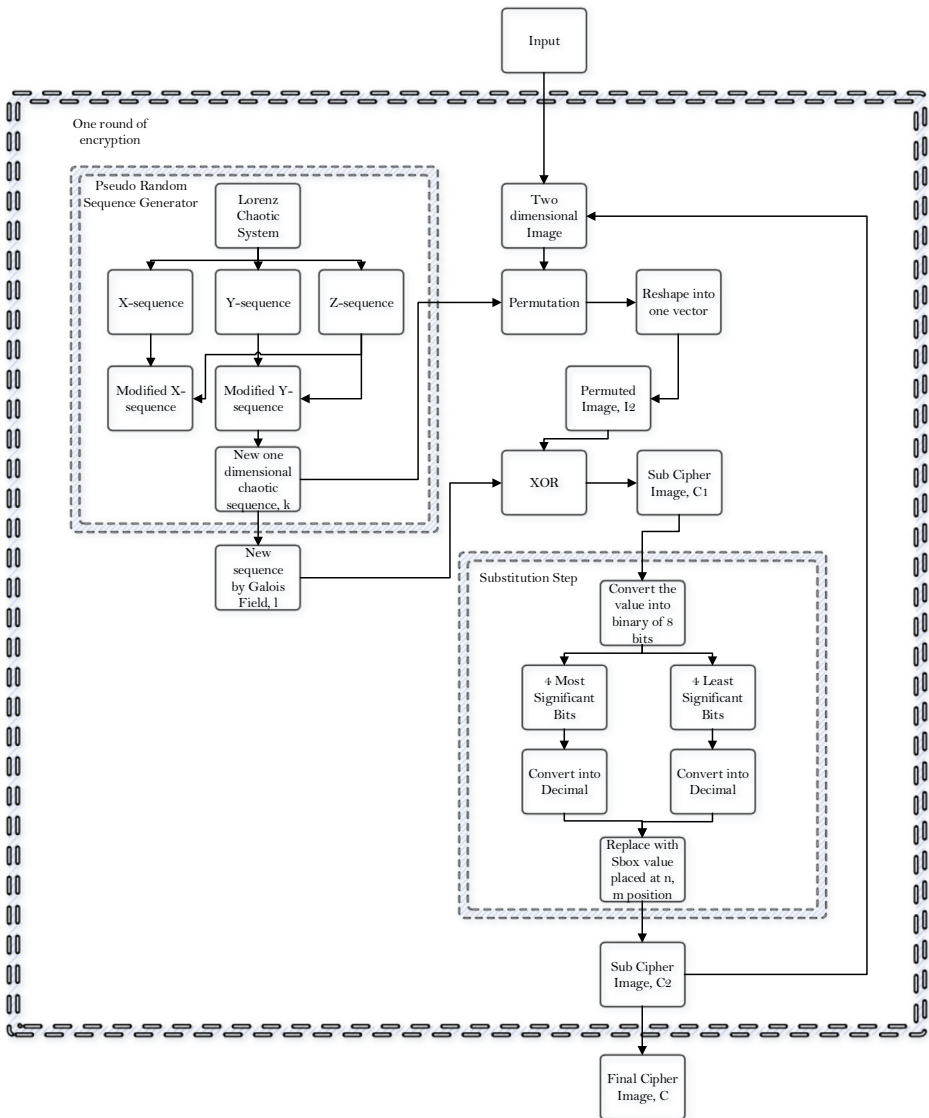


Fig. 1 Flowchart of the proposed algorithm

and histogram of cameraman are depicted in Fig. 2a and c. Figure 2a undergoes the process of encryption through our proposed encryption scheme and the encrypted image is given in Fig. 2b. The strong visual results of encrypted image indicate the quality of encryption algorithm. Furthermore, the histogram of encrypted image in Fig. 2d also confirms the strength of our scheme. On the other hand, the proposed image encryption scheme is applied on gray scale image having gray value of 124. The gray scale image is given in Fig. 3a and b represents the encrypted image of the gray scale image. Moreover, Fig. 3c and d depicts the histogram images of plaintext image and encrypted image respectively. The results of

Table 4 The initial conditions of chaotic maps used as secret keys in the proposed encryption technique

Parameters	a	b	c
	10	28	8/3

encryption are satisfactory regardless of high autocorrelation in the plain image. Similarly, the histogram of the encrypted gray scale image shows strength of our proposed technique.

5.1 Statistical analysis

The statistical analyses are used to evaluate the strength of proposed image encryption technique. In this work, we have employed different statistical analyses to determine the standard of our proposed image encryption technique. In addition to this, the results of proposed technique are being compared with the results of well-known image encryption techniques. The description of these analyses is given in the following subsections.

5.1.1 Correlation

The correlation of an image is given as [5, 26]:

$$Corr. = \sum_{i,j} \frac{(i - \mu_i)(j - \mu_j)\rho(i, j)}{\varphi_i\varphi_j}. \quad (44)$$

where (i, j) corresponds to image pixels positions, $(\rho(i, j))$ is pixel value at (i^{th}) row and (j^{th}) column of image, μ is the variance, φ is the standard deviation. The correlation analysis determines the similarity between two neighbor image pixels over the whole image having range between $[-1, 1]$ with 1 showing the perfect correlation.

Figure 4a shows the distribution of horizontally adjacent pixels of cameraman image and Fig. 4b shows the distribution of horizontally adjacent pixels of encrypted cameraman image. The distribution of vertical adjacent pixels in ciphered cameraman image will act similar as they respond in horizontal adjacent pixels.

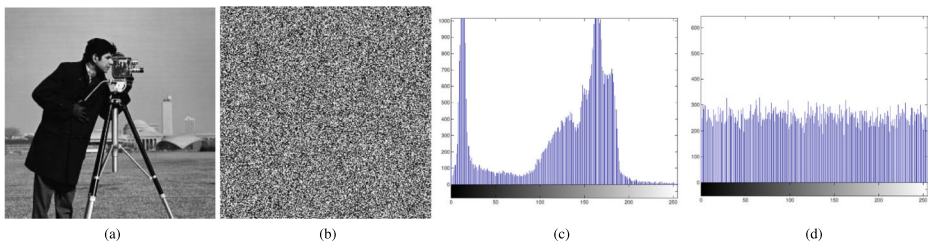


Fig. 2 Simulation outcomes of proposed scheme **a** 256×256 size plain image of cameraman **b** cameraman image after encryption with secret keys **c** histogram analysis of cameraman **d** histogram analysis of encrypted cameraman

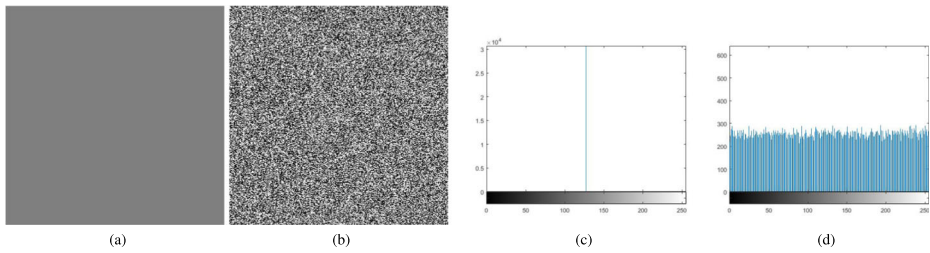


Fig. 3 Simulation outcomes of new image encryption technique. **a** gray scale image having size 256×256 , **b** encrypted image of gray scale **c** histogram results of one gray scale image **d** histogram results of encrypted one gray scale image

5.1.2 Entropy

The entropy of an image is given as [5, 26]:

$$Entropy = - \sum_{i,j} pr(\rho(i, j)) \log_2 pr(\rho(i, j)). \tag{45}$$

where i, j corresponds to image pixels positions, $\rho(i, j)$ is pixel value at i^{th} row and j^{th} column of image and $pr(\rho(i, j))$ is the probability of image pixel. Entropy shows the randomness of image having range between $[0 \ 8]$ for an image having 256 gray scales. A greater value of entropy shows the greater amount of randomness.

5.1.3 Contrast

The contrast of an image is given as [5, 26]:

$$Contrast = \sum_{i,j} |i - j|^2 \rho(i, j). \tag{46}$$

where i, j corresponds to image pixels positions, $\rho(i, j)$ is pixel value at i^{th} row and j^{th} column of image. The contrast analysis of the image enables the viewer to vividly identify

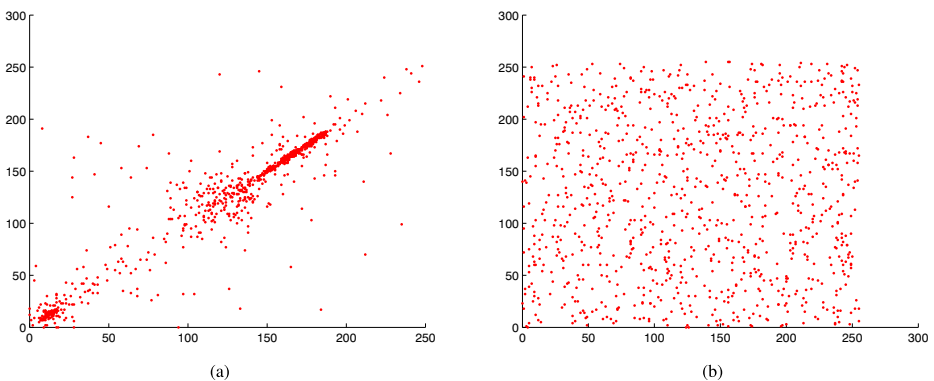


Fig. 4 a The distribution of horizontally adjacent pixels of cameraman image and **b** encrypted cameraman image. The distribution of vertical adjacent pixels ciphered cameraman image will behave the same as horizontal adjacent pixels

the objects in texture of an image. The contrast values ranges from $[0 (size(Image) - 1)^2]$. The contrast value of a constant image is 0. The greater value of the contrast shows greater variation in image pixels.

5.1.4 Homogeneity

In [5, 26], the homogeneity of image is defined as:

$$Homo. = \sum_{i,j} \frac{\rho(i, j)}{1 + |i - j|}. \quad (47)$$

where the location of image pixels is given by i, j . In this analysis, the closeness of gray level cooccurrence matrix (GLCM) diagonal and GLCM is calculated. The interval for homogeneity is $[0 1]$.

5.1.5 Energy

The energy of an image can be defined as [5, 26]:

$$Energy = \sum_{i,j} \rho(i, j)^2. \quad (48)$$

where i, j depicts the position of image pixels. The above equation interprets the energy analysis as the summation of square of all elements in GLCM. The value of energy lies in the interval $[0 1]$ and the constant image has maximum energy value of 1. Table 5 shows the value of energy analysis and also the comparison with other existing techniques. This comparison indicates the quality of our proposed scheme.

6 Security analysis

It is mandatory to compute the security analyses to assess the strength of any cryptosystem. In this section, we assessed the security of our scheme with the help of certain security analyses like key space, key sensitivity, avalanche analysis, noise resistant analysis and cryptanalysis. The comparison of the outcomes of these analyses with the security analyses of other schemes exemplify the strength of our proposed technique. Following sections describe the security analyses in detail.

Table 5 Comparative statistical analysis on the encrypted images of lena resulted from applying proposed image encryption algorithm and other related works

Analysis	Corr.	Entropy	Homo.	Contrast	Energy
Ref. [32]	0.0687	7.1735	0.8121	8.3849	0.1254
Ref. [4]	0.0439	2.5643	0.5733	4.9454	0.4263
Ref. [42]	0.0313	7.9735	0.8251	8.1833	0.2132
Ref. [38]	-0.0308	7.9311	0.8365	8.0522	0.1984
Ref. [1]	-0.0293	7.9801	0.9102	8.6603	0.0674
Ref. [15]	0.0025	7.9972	0.8742	8.4251	0.0257
Proposed	-3e-4	7.9521	0.9598	8.4587	0.3521

6.1 Key space and key sensitivity

For any cryptographic system, the total number of secret keys which are used to encrypt the data are named as key space and it has its importance as far as security of whole scheme is concerned. In this work, the secret keys are the initial conditions of three different chaotic maps. The secret key has average range of 10^{20} and we have used three different secret keys so the total number of different keys can be given as $10^{20 \times 3} = 10^{60}$. A recent personal computer will require over 10^{10} years to go through all possible blends of this huge keyspace.

One of the features of the quality cryptosystem is there sensitivity to a tiny change in secret keys. For instance, the change in secret key during decoding process will give altogether a different decoded image. This mechanism is named as key sensitivity. Our proposed encryption technique is sensitive to even a minor change in the initial conditions. To prove this claim, we will change the secret keys and show the pictorial results. By using secret keys as mentioned in Table 2, we have encrypted the cameraman image as given in Fig. 2a. Considering four different cases of changing initial secret keys we have following results.

- Case I:** If the initial secret key k_1 is slightly changed i.e., $k_1 = a = 10$ to $k'_1 = a = 10.0000000001$ then it is observed that the decryption process does not get the required results. Figure 5a depicts the decryption of plain-image with key k'_1 . In this process, the remaining two keys were remained the same.
- Case II:** For the second case, the key k_2 is changed from its original value i.e., $k_2 = b = 28$ to $k'_2 = b = 28.0000000001$ and again with this slight change in one key, the decryption image does not resemble to the original plaintext image and hence prove our claim of key sensitivity. The decryption is given in Fig. 5b.
- Case III:** The initial secret key k_3 is slightly changed while keeping the remaining keys same. A change of 0.0000000001 in k_3 i.e $k_3 = c = 8/3$ to $k'_3 = c = 8/3 + 0.0000000001$ provides a different original image as given in Fig. 5c.
- Case IV:** For the last case, the key k_4 is changed like $k_1 = a = 10$ to $k'_1 = a = 9.9999999999$ and the decrypted image is given in Fig. 5d.

In all four cases, even a slight change in the initial secret key could not obtain the original image and hence prove our claim of key sensitivity for proposed algorithm.

6.2 Avalanche analysis

In block ciphers, the effect of avalanche mentions one of the properties of strong cryptographic algorithms. If a single input bit change effect the half number of output bits, then it is an apparent avalanche effect. Researchers prefer unified average change intensity (UACI) and number of pixel change rate (NPCR) to measure the effect of avalanche criteria. The detailed description of this effect is provide in [43] as:

$$NPCR = \frac{\sum_{i,j} D(i, j)}{N \times M} \times 100\%, \tag{49}$$

$$UACI = \frac{1}{N \times M} \left[\sum_{i,j} \frac{|C_1(i, j) - C_2(i, j)|}{255} \right] \times 100\%, \tag{50}$$

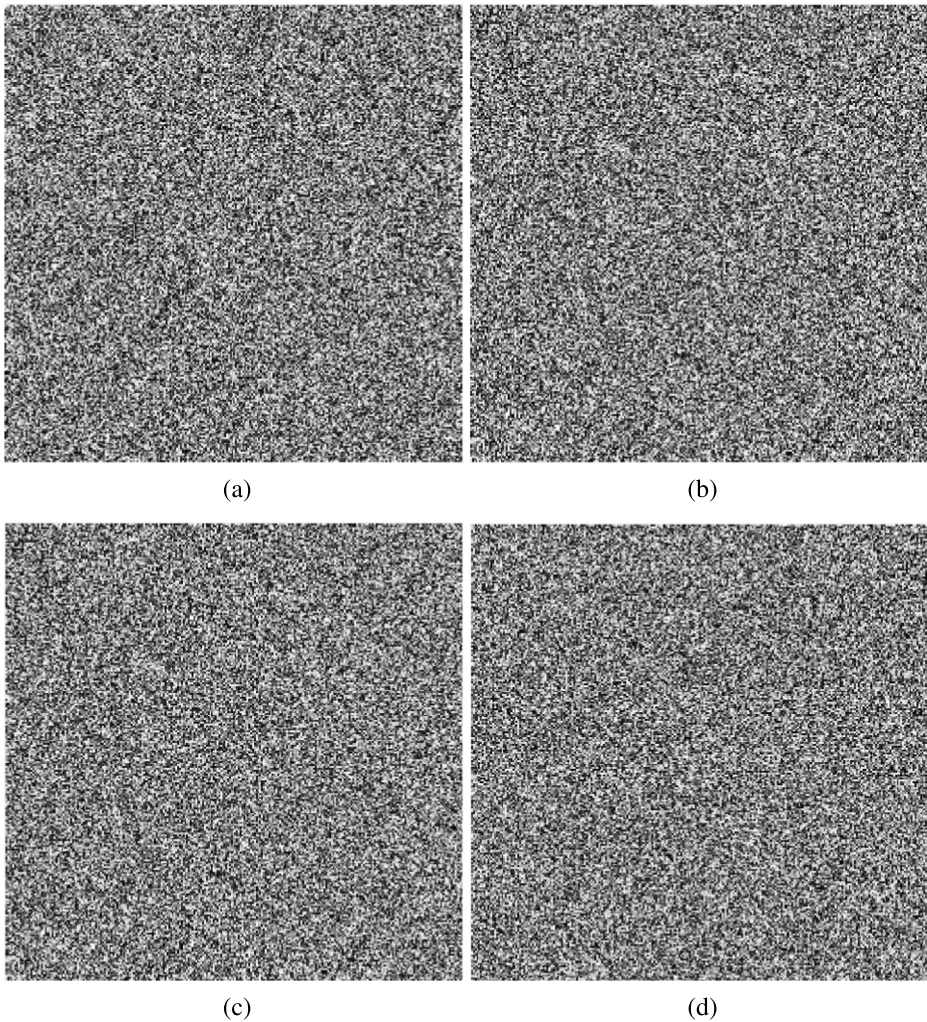


Fig. 5 Key sensitivity analysis **a** First secret key is changed from $k_1 = a = 10$ to $k'_1 = a = 10.0000000001$ **b** Second secret key is $k_2 = b = 28$ to $k'_2 = b = 28.0000000001$ **c** Third secret key is changed from $k_3 = c = 8/3$ to $k'_3 = c = 8/3 + 0.0000000001$ **d** Fourth secret key is changed from $k_1 = a = 10$ to $k'_1 = a = 9.9999999999$

Where the two ciphered digital images C_1 and C_2 are attained by changing the single bit of plain image. Moreover, the height and width of cipher images are given by N and M respectively. We can define the $D(i, j)$ as

$$D(i, j) = \begin{cases} 0 & \text{if } C_1(i, j) = C_2(i, j), \\ 1 & \text{if } C_1(i, j) \neq C_2(i, j). \end{cases}$$

By adjusting the single pixel of plaintext image, the rate of change of pixel quantity of encrypted image is measured by number of pixel change rate (NPCR) analysis. Moreover, the normal power of contrast between plain and encrypted images is calculated by unified average change intensity analysis (UACI). The calculated minimum value for NPCR must

be 50 percent. In our work, three different plain images of Lena, baboon and cameraman have been through NPCR and UACI analyses. For each image, the position of bit is firstly changed around first pixel then around middle pixel and finally around the last pixel. Table 6 depicts the outcomes of NPCR and UACI for all cases of three images. In this Table, the value of NPCR remains greater than 99 percent and value of UACI is greater than 33 percent. These results indicate the strong avalanche effects. In addition to this, a comparison has been established between avalanche values of proposed scheme and AES

By using NPCR and UACI analyses, the key sensitivity of proposed scheme is also evaluated. In first case, two same keys with difference of only 1 bit are used to calculate the difference between two encrypted images. For the second case, the difference of one bit between two keys would remain the same but we calculated the difference between encrypted and decrypted images. Table 6 gives the results of both cases along with comparison with AES. The results of Table 6 show the required avalanche effect.

6.3 Noise resistant analysis

The noise resistant encryption algorithm depicts the strength of any cryptosystem. Any transmitted data may get effected by channel (irrespective of wired or wireless channel) noise or deliberately added noise. It is observed that it is hard to decipher the abandoned cipher image even the portion of the image is affected. Few methods like error detection and correction have been used to counter these situations but at the cost of computational complexity. For successful transmission and decryption of cipher data, the error detection and correction are required before both the steps. So, ultimately it increases the complexity of the system. In this proposed technique, the addition of noise does not become the hurdle to decipher image correctly with some minor changes. To verify this claim, a series of experiments regarding successful deciphering have been done with noise addition in the cipher images. Figure 6a and b represent the plain image and encrypted images respectively. This

Table 6 The comparison of UACI and NPCR analysis of proposed technique and AES on the images of Lena, Baboon and cameraman. For all three images three cases are proposed. Changing of single bit in first pixel, mid pixel and last pixel. Moreover, the analysis of key sensitivity for two cases are also given

Analysis		NPCR(%)		UACI(%)		
		Prop.	AES	Prop.	AES	
Images & Loc.						
	Cman	first	99.5212	99.6048	33.5120	33.5360
		mid	99.5862	99.6201	33.3014	33.5212
		last	99.5410	99.5819	33.4120	33.5245
Lena		first	99.2563	99.6094	33.2010	33.3996
		mid	99.5210	99.6506	33.6320	33.3139
		last	99.4198	99.6002	33.5202	33.5133
Baboon		first	99.1252	99.6124	33.3620	33.4463
		mid	99.5271	99.6033	33.4510	33.4561
		last	99.6389	99.6185	33.6930	33.5252
Key S.	Case I		99.4802	99.5972	33.7401	33.5029
	Case II		99.0025	99.6460	33.2015	33.5468

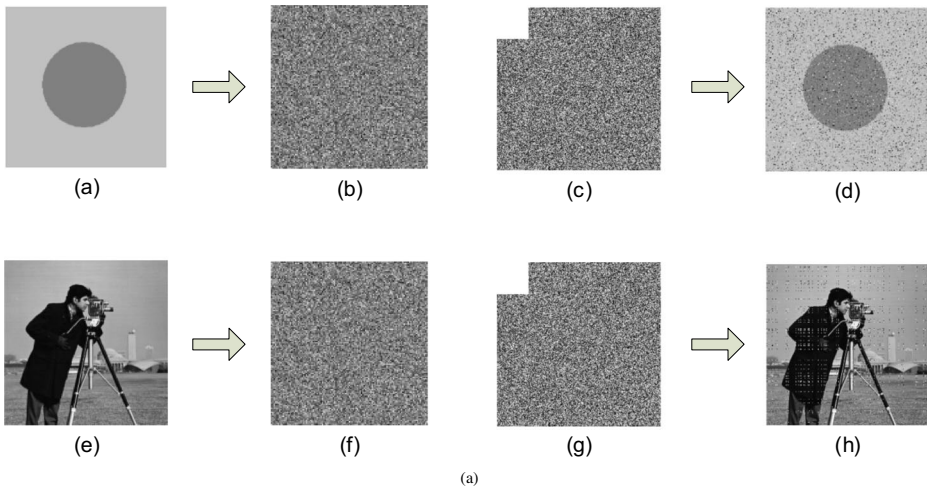


Fig. 6 **a** A test image, **b** encryption of test image using secret keys. **c** Adding noise in the cipher image by changing first 10,000 pixels either by cropping or corrupting the file by using the white pixels. **d** Deciphered image. **e** The cameraman noisy image, **f** encryption of cameraman image using secret keys. **g** Adding noise in the cipher image by changing first 10,000 pixels either by cropping or corrupting the file by using the white pixels. After decryption, **h** Deciphered image

encryption is done with the help of secret keys of Table 4. For noise resistance test, the 10,000 pixels of encrypted image are either cropped or made corrupted with white pixels as shown in Fig. 6c. The deciphering of this image is given in Fig. 6d. Clearly, this pictorial representation indicates the successful decryption with minor changes. To prove this claim for other images, the cameraman image is encrypted with the secret keys of Table 4. The plain image with noise and its encryption is given in Fig. 6e and f respectively. Now, again we removed first 10,000 pixels either with the help of cropping or by corrupting the image. Interestingly, the decryption is successful with minor changes and as shown in Fig. 6g and h.

On the other hand, there is a difference between the deciphering of plain text and digital image. For noisy cipher text, the deciphering of the text gives a whole new text. There are many examples in which the major concern is to recognize the face of the person and object irrespective of quality of decipher images. For this reason, the deciphering of encrypted images having added noise is major breakthrough.

6.4 Cryptanalysis

To evaluate the strength of proposed scheme against different malicious attacks, following attacks are considered to evaluate the proposed cryptosystem.

6.4.1 Linear cryptanalysis

Linear approximation probability is used to analyze the imbalance of an event. The maximum value of imbalance of the event can also be obtained with the help of this analysis. In this analysis, two masks Γx and Γy , are applied to parity of both input and output bits, respectively. In [25], it is defined as:

$$LP = \max_{\Gamma x \Gamma y \neq 0} \left| \frac{\{x/X \bullet \Gamma x = S(x) \bullet \Gamma y = \Delta y\}}{2^n} - \frac{1}{2} \right|, \quad (51)$$

where all the inputs values are contained by set X and total number of this set are 2^n . As we have used 8 different S-boxes and the average maximum value of LP is $LP_{\max} = 2^{-4.21}$ and having distinct 256 S-boxes the maximum LP is given as $LP_{\max}^{4r} = 2^{-4.21 \times 256} = 2^{-1077}$. By seeing the outcomes of LP, it is almost impossible for an invader to differentiate our proposed cipher with the help of random permutation and hence, the proposed algorithm will show resistance for countering linear cryptanalysis.

6.4.2 Differential cryptanalysis

One of the precise goals for assurance of uniform mapping, the input differential extraordinarily supervises the differential at output end. These features certify the probability of uniform mapping for every input bit i . The main purpose of approximation probability is to calculate differential uniformity of S-box. In [8] it is given as:

$$DP(\Delta x \rightarrow \Delta y) = \left[\frac{\{x \in X/S(x) \oplus S(x \oplus \Delta x) = \Delta y\}}{2^m} \right], \tag{52}$$

where the input and output differentials are given by Δx and Δy respectively. For S-boxes, the maximum average value of DP is $DP_{\max} = 2^{-4.05}$. Here, the number of active S-boxes is exactly 256 i.e., $DP_{\max}^{4r} = 2^{-4.05 \times 256} = 2^{-1036}$. By seeing this outcome, it is confirmed that proposed scheme has the ability to resist against malicious differential cryptanalysis.

Moreover, we have done the security analysis of the proposed substitution box and compared with the state-of-art recent works. Table 7 shows the comparative results strict avalanche criterion, bit independent criterion, BIC for SAC, linear approximation probability, and differential approximation probability of proposed and other S-boxes demonstrating the superiority of our proposed S-Box.

6.5 Computational time

The other requirement for the encryption algorithm is the computational complexity, which is required to be as minimum as possible for the effective and efficient implementation of encryption algorithm over the different platforms. We have computed the time required for the proposed encryption algorithm considering 12 rounds and a data block size of 20 MB. We have compared the computational time of the proposed algorithm and compared with the state-of-art recent works. Table 8 shows the comparative results of computational

Table 7 Comparative analysis of strict avalanche criterion, bit independent criterion, BIC for SAC, linear approximation probability, and differential approximation probability of proposed and other S-boxes

Methods	SAC	BIC	BIC of SAC	LP	DP
Ref. [7]	0.4998	112	0.504	144/0.0625	0.0156
Ref. [12]	0.4999	112	0.504	144/0.0625	0.0156
Ref. [19]	0.4864	104	0.504	144/0.1563	0.0172
Ref. [37]	0.4939	107	0.504	160/0.0625	0.0625
Ref. [37]	0.5020	103	0.505	160/0.1250	0.0469
Ref. [37]	0.5040	112	0.504	144/0.0625	0.0156
Ref. [37]	0.5040	112	0.504	144/0.0625	0.0156
Ref. [37]	0.5040	112	0.504	144/0.0625	0.0156
Proposed	0.4999	112	0.504	144/0.0625	0.0156

Table 8 Comparative results of computational time of proposed and other works demonstrating the superiority of our proposed work

Methods	Computational Time (sec)
Ref. [7]	12
Ref. [12]	21
Ref. [19]	17
Ref. [37]	14
Proposed	3.7

time of proposed and other works demonstrating the superiority of our proposed work. The time is computed on a desktop machine using MATLAB software on Windows 10 with i5 processor and 8GB RAM.

7 Conclusion

In this paper, combination of proposed S-boxes and chaotic maps is used for image encryption algorithm. This scheme consists of two phases. In the first phase, substitution is performed by using multiple S-boxes instead a single S-box. The application of several S-boxes not only provide Additional security but also utilizes less round of encryption. The initial values of Lorenz chaotic map help to operate each round of encryption. In addition to this, permutation is performed in the second phase. The resistance of proposed encryption scheme is depicted through simulation and security analyses results. The outcomes of cryptanalysis also confirm the robustness of our proposed scheme. This work also motivates researchers to add different changes like increasing number of S-boxes and encryption rounds by keeping standard of encryption and computational complexity.

Funding Open access funding provided by the Qatar National Library.

Open Access This article is licensed under a Creative Commons Attribution 4.0 International License, which permits use, sharing, adaptation, distribution and reproduction in any medium or format, as long as you give appropriate credit to the original author(s) and the source, provide a link to the Creative Commons licence, and indicate if changes were made. The images or other third party material in this article are included in the article's Creative Commons licence, unless indicated otherwise in a credit line to the material. If material is not included in the article's Creative Commons licence and your intended use is not permitted by statutory regulation or exceeds the permitted use, you will need to obtain permission directly from the copyright holder. To view a copy of this licence, visit <http://creativecommons.org/licenses/by/4.0/>.

References

1. Ahmad J, Hwang SO (2015) Chaos-based diffusion for highly autocorrelated data in encryption algorithms. *Nonlinear Dynamics* 82(4):1839–1850
2. Alvarez G, Li S (2006) Some basic cryptographic requirements for chaos-based cryptosystems. *Int J Bifurcation Chaos* 16(08):2129–51
3. Amigo JM, Kocarev L, Szczepanski J (2007) Theory and practice of chaotic cryptography. *Phys Lett Section A* 366(3):211–16. <https://doi.org/10.1016/j.physleta.2007.02.021>
4. Anees A, Siddiqui AM, Ahmed F (2014) Chaotic substitution for highly autocorrelated data in encryption algorithm. *Commun Nonlinear Sci Numer Simul* 19(9):3106–3118

5. Anees A, Siddiqui AM, Ahmed J, Hussain I (2014) A technique for digital steganography using chaotic maps. *Nonlinear Dynamics* 75(4):807–816
6. Bakhache B, Ghazal JM, El Assad S (2014) Improvement of the security of zigbee by a new chaotic algorithm. *IEEE Syst J* 8(4):1021–30. <https://doi.org/10.1109/JSYST.2013.2246011>
7. Belazi M, E-Latif AAA, Belghith S (2017) Khan efficient cryptosystem approaches: S-boxes and permutation-substitution-based encryption. *Wirel Pers Commun* 87(1):337–361
8. Biham E, Shamir A (1993) *Differential cryptanalysis of the data encryption standard*. Springer
9. Çavuşoğlu U, Akgül A, Kaçar S, Pehlivan İ, Zengin A (2016) A novel chaos-based encryption algorithm over TCP data packet for secure communication. *Secur Commun Netw* 9(22):5968–74
10. Chen G, Mao Y, Chui CK (2004) A symmetric image encryption scheme based on 3D chaotic cat maps. *Chaos Solitons Fractals* 21(3):749–61. <https://doi.org/10.1016/j.chaos.2003.12.022>
11. Cicek S, Uyaroğlu Y, Pehlivan I (2013) Simulation and circuit implementation of sprott case h chaotic system and its synchronization application for secure communication systems. *J Circuits Syst Comput* 22(04):1350022
12. Daemen J, Rijmen V (2002) *The design of Rijndael: AES - The advanced encryption standard*. Springer
13. Dillak RY (2013) Digital color image encryption using RC4 stream cipher and chaotic logistic map. *Information Technology and Electrical Engineering (ICITEE), 2013 International Conference on*
14. Farah MAB, Kachouri A, Samet M (2011) Improvement of cryptosystem based on iterating chaotic map. *Commun Nonlinear Sci Numer Simul* 16(6):2543–2553
15. Guesmi R, Farah MAB (2021) A new efficient medical image cipher based on hybrid chaotic map and DNA code. *Multimed Tools Appl* 80:1925–1944
16. Hussain I (2013) A projective general linear group based algorithm for the construction of substitution box for block ciphers. *Neural Computing & Applications* 22:1085–1093
17. Jakimoski G, Kocarev L (2001) Chaos and cryptography: block encryption ciphers based on chaotic maps. *IEEE Trans Circuits Syst I* 48(2):163–9. <https://doi.org/10.1109/81.904880>
18. Jolfaei A, Mirghadri A (2011) Image encryption using chaos and block cipher. *Comput Inf Sci* 4(1):172–85. www.ccsenet.org/cis
19. Khan M, Shah T, Batool SI (2016) Construction of S-box based on chaotic Boolean functions and its application in image encryption. *Neural Comput and Applic* 27(3):667–685
20. Kohli R, KKumar M (2013) Optimized on system analysis using AES and X-tea. *IJARCSSE* 3(2). ISSN 2277-128X
21. Kohli R, Sharma D, Baliyan MK (2012) S-Box design analysis and parameter variation in AES algorithm. *Int J Comput Appl* 60(2)
22. Li S, Mou X, Cai Y (2001) Pseudo-random bit generator based on couple chaotic systems and its applications in stream-cipher cryptography. *Proceedings, Lecture Notes in Computer Science* 2247:316–329
23. Liu H, Kadir A, Niu Y (2014) Chaos-based color image block encryption scheme using S-box. *AEU - Int J Electr Commun* 68(7):676–86. <https://doi.org/10.1016/j.aeu.2014.02.002>
24. Liu Y, Tian S, Hu W, Xing C (2012) Design and statistical analysis of a new chaotic block cipher for wireless sensor networks. *Commun Nonlinear Sci Numer Simul* 17(8):3267–78. <https://doi.org/10.1016/j.cnsns.2011.11.040>
25. Matsui M (1994) Linear cryptanalysis of the data encryption standard. In: *Eurocrypt'93, LNCS, vol 765*. Springer, pp 386–397
26. Morioka S (2002) An optimized S-box circuit architecture for low power AES design. *Workshop on cryptographic hardware and embedded systems, CHES.02*. In: *LNCS, vol 2523*, pp 172–186
27. Noura H, El Assad S, Vladeanu C (2010) Design of a fast and robust chaos-based crypto-system for image encryption. In: *2010 8th international conference on communications, COMM 2010*, pp 423–6. <https://doi.org/10.1109/ICCOMM.2010.5509114>
28. Ott E (1979) *Chaos in dynamical systems*. Second edition
29. Ozkaynak F, Yavuz S (2013) Designing chaotic S-boxes based on time-delay chaotic system. *Nonlinear Dyn* 74(3):551–7. <https://doi.org/10.1007/s11071-013-0987-4>
30. Pareschi F, Setti G, Rovatti R (2010) Implementation and testing of high-Speed CMOS true random number generators based on chaotic systems. *IEEE Trans Circuits Syst I* 57(12):3124–37. <https://doi.org/10.1109/TCSL.2010.2052515>
31. Pehlivan I, Wei Z (2012) Analysis, nonlinear control, and chaos generator circuit of another strange chaotic system. *Turk J Electr Eng Comput Sci* 20(SUPPL.2):1229–39. <https://doi.org/10.3906/elk-1103-14>
32. Pisarchika AN, Zanin M (2008) Image encryption with chaotically coupled chaotic maps. *Physica D: Nonlinear Phenomena* 237(20):2638–2648
33. Rhouma R, Solak E, Belghith S (2010) Cryptanalysis of a new substitution-diffusionbased image cipher. *Commun Nonlinear Sci Numer Simul* 15(7):1887–92. <https://doi.org/10.1016/j.cnsns.2009.07.007>

34. Solak E, Çokal C, Yildiz OT, BIYIKOG LU T (2010) Cryptanalysis of Fridrich chaotic image encryption. *Int J Bifurcation Chaos* 20(05):1405–13
35. Tang G, Liao X (2005) A method for designing dynamical S-boxes based on discretized chaotic map. *Chaos Solitons Fractals* 23(5):1901–9. <https://doi.org/10.1016/j.chaos.2004.07.033>
36. Tang G, Liao X, Chen Y (2005) A novel method for designing S-boxes based on chaotic maps. *Chaos Solitons Fractals* 23(2):413–19. <https://doi.org/10.1016/j.chaos.2004.04.023>, <http://www.sciencedirect.com/science/article/pii/S0960077904002474>
37. Ullah SS, Shah T (2017) Jamal A novel construction of substitution box using a combination of chaotic maps with improved chaotic range. *Nonlinear Dynamics* 88(4):2757–2769
38. Wang X, Teng L, Qin X (2012) A novel colour image encryption algorithm based on chaos. *Signal Process* 92(4):1101–1108
39. Wang Y, Wong K-W, Liao X, Chen G (2011) A new chaos-based fast image encryption algorithm. *Appl Soft Comput* 11(1):514–22. <https://doi.org/10.1016/j.asoc.2009.12.011>
40. Wang Y, Wong KW, Liao X, Xiang T (2009a) A block cipher with dynamic S-boxes based on tent map. *Commun Nonlinear Sci Numer Simul* 14(7):3089–99. <https://doi.org/10.1016/j.cnsns.2008.12.005>
41. Wang Y, Xie Q, Wu Y, Du B (2009b) A software for S-box performance analysis and test. In: *Proceedings - 2009 International conference on electronic commerce and business intelligence, ECBI 2009*, p 125–8. <https://doi.org/10.1109/ECBI.2009.15>
42. Wang X-Y, Yang L, Liu R, Kadir A (2010) A chaotic image encryption algorithm based on perceptron model. *Nonlinear Dynamics* 62(3):615–621
43. Wu Y, Noonan JP, Ağaian S (2010) NPCR and UACI randomness tests for image encryption. *Cyber Journals: Multidisciplinary journals in science and technology, Journal of selected areas in telecommunications*, pp 31–38
44. Yang D, Liao X, Wang Y, Yang H, Wei P (2009) A novel chaotic block cryptosystem based on iterating map with output-feedback. *Chaos Solitons Fractals* 41(1):505–10. <https://doi.org/10.1016/j.chaos.2008.02.017>
45. Yang H, Wong K-W, Liao X, Zhang W, Wei P (2010) A fast image encryption and authentication scheme based on chaotic maps. *Commun Nonlinear Sci Numer Simul* 15(11):3507–17. <https://doi.org/10.1016/j.cnsns.2010.01.004>
46. Zhang Y (2013) Encryption speed improvement on an improvement over an image encryption method based on total shuffling. In: *Proceedings of 2013 International conference on sensor network security technology and privacy communication system, Nangang, China*

Publisher's note Springer Nature remains neutral with regard to jurisdictional claims in published maps and institutional affiliations.